Journal of Non-Crystalline Solids 511 (2019) 201–211

Contents lists available at ScienceDirect

Journal of Non-Crystalline Solids

journal homepage: www.elsevier.com/locate/jnoncrysol

Reducing crystallinity on thin film based CMC/PVA hybrid polymer for application as a host in polymer electrolytes

M.A. Saadiah[a,c], D. Zhang[b], Y. Nagao[b], S.K. Muzakir[c], A.S. Samsudin[c,*]

[a] Department of Chemistry, Centre for Foundation Studies, International Islamic University Malaysia, 26300, Gambang, Pahang, Malaysia
[b] School of Materials Science, Japan Advanced Institute of Science and Technology, 1-1 Asahidai, Nomi, Ishikawa 923-1292, Japan
[c] Ionic Materials Team, Advanced Material, Faculty of Industrial Sciences & Technology, Universiti Malaysia Pahang, Lebuhraya Tun Razak, 26300, Kuantan, Pahang, Malaysia

ARTICLE INFO

Keywords:
Carboxymethyl cellulose/polyvinyl alcohol
Hybrid polymer blend
Structural properties
Conductivity

ABSTRACT

The carboxymethyl cellulose and polyvinyl alcohol (CMC/PVA) based hybrid polymer (HPe) system with different ratio of composition have been prepared via solution casting. The features of interaction between CMC and PVA were investigated using X-ray diffraction (XRD), and infrared (IR) spectroscopy to disclose the reduction of crystallinity of the HPe system. Morphological properties observed by Scanning electron microscopy (SEM) confirmed the homogeneity of the HPe system. Differential scanning calorimetry (DSC) result explains the miscibility of the HPe system which was confirmed by means of variations in the glass transition temperature (T_g). Two degradation mechanisms were revealed by thermogravimetric analysis (TGA) in the HPe system attributed to the decarboxylation in CMC and degradation of bond scission in PVA backbone. The blend of 80:20 compositions of CMC/PVA HPe system was found to be the optimum ratio with an increase in conductivity of CMC/PVA by one magnitude order from 10^{-7} to 10^{-6} S/cm with the lowest in crystallinity.

1. Introduction

Advancement of more efficient energy storage devices employing the polymer electrolyte (PE) has emerged as powerful platforms. PE based solid form is a key material for all-solid-state energy devices which are known as the key of many electrochemical devices [1–3]. For these reasons, numerous efforts have been considered during the development of solid polymer electrolyte including the application of petroleum-based polymer or renewable bio-polymer based. Extensive study has been focusing on the application of petroleum-based polymers which give disadvantages such as high cost, depletion of petroleum resources and trigger environmental problems.

Recently, the use of biopolymer material has raised special attention as they are abundant in nature and eco-friendlier. The growing interest in biodegradable materials has aggravated the researchers to study extensively as polymer electrolyte system. Several renewable resource of polymer are suitable to act as host polymer including chitosan [4,5], carrageenan [6–8], polylactides [9], agarose [10,11] and carboxymethyl cellulose [12] which are favorable in the preparation of polymer electrolytes. Carboxymethyl cellulose (CMC) is regarded as the most important classification of polysaccharide. CMC is a biodegradable material, low-cost material to be produced, non-toxic to environment, semi-crystalline material and exhibit excellent film forming ability but lack of strength and low in conductivity [12]. Large number of works has been reported on the application of CMC as a single polymer electrolyte system, however, due to exceptionally stiff behavior, small elongation at break (less than 8%) and trigger the problem in the electrochemical stability which is not well-suited especially in the application of electrochemical devices [13]. On top of that, the properties of single polymer may not offer outstanding physical and mechanical or chemical properties to accommodate wide range especially in energy storage device applications.

Thus, blending method, which is incorporation with other polymer, becomes an alternative method which can alter the structural and electrical properties and therefore widen their fields of application [14,15]. According to Rudzhiah et al. [6] the incorporation of CMC into carrageenan has proved that blending can manipulate the structure of the polymer and increase the conductivity via the formation of H-bonding. Blending method study has been focusing on intermolecular complexation in governing the enhancement of amorphousness and conductivity [16]. Tremendous study on hybrid polymer system has been carried out including starch/chitosan [14,17], carboxymethyl cellulose (CMC)/chitosan [18], starch/chitosan and polyvinyl alcohol (PVA)/ polyethylene oxide (PEO) [19]. Incorporation of bio-polymer

* Corresponding author.
E-mail address: ahmadsalihin@ump.edu.my (A.S. Samsudin).

https://doi.org/10.1016/j.jnoncrysol.2018.11.032
Received 13 August 2018; Received in revised form 26 November 2018; Accepted 27 November 2018

becomes favorable due to their special characteristic which is renewable, non-toxic and ease in preparation. As a result, many studies on hybrid polymer using natural resources are conducted in order to achieve excellent conductivity.

The present work based on the attempt to produce a novel favorable electrochemical properties of carbohydrate polymer namely carboxymethyl cellulose (CMC) by adopting the blending technique with addition of polyvinyl alcohol (PVA) in order to produce hybrid polymer (HPe) system. PVA is known a water-soluble polymer prepared by partial or complete hydrolysis of polyvinyl acetate. It is non-toxic as well as degradable with high tensile strength and flexibility [20]. In the present work, structural, thermal and optical properties of CMC-PVA complex were investigated via FTIR, XRD, SEM, TGA, and DSC. Besides, the conductivity of the HPe system was investigated via EIS in order to identify the effect of blending. The investigation from the novel present work would create an opportunity as a step in the expansion of doping and plasticized system which to be used as polymer host in polymer electrolytes.

2. Experimental

2.1. HPe film preparation

CMC (molecular weight: 90000; Acros Organic Co.) and partially hydrolyzed PVA ~85% (molecular weight: 70000; Merck Schucardt) were used in this present work. The CMC/PVA hybrid polymer was prepared by a solution casting technique. Various percentage of CMC/PVA composition was dissolved in distilled water. The mixed solution was casting into glass petri dishes followed by oven drying for about 300 min at 60 °C and accompanied by further drying in desiccator to ensure all solvent has been evaporated. Fig. 1 shows the schematic preparation, thin film appearance, chemical structure and blended composition of HPe system.

2.2. Characterization of CMC/PVA HPe system

2.2.1. Scanning electron microscopy (SEM)

Surface morphological analysis of the HPe system was investigated using Tabletop Miniscope TM3030Plus (Hitachi High Technologies, Japan) equipped with an energy dispersive X-ray spectrometer (EDS). An accelerating voltage of 10 kV and 15 kV were used for SEM and EDX respectively. Charge-up reduction mode was used.

2.2.2. Infrared (IR) spectroscopy

2.2.2.1. Attenuated total reflection-Fourier transforms infrared (ATR-FTIR). The complexation between CMC/PVA was investigated using Perkin Elmer FTIR spectrophotometer equipped with an attenuated total reflection (ATR) in the frequency range of 700 cm^{-1} to 4000 cm^{-1}. All ATR-FTIR spectra were obtained at 10 scans with a resolution of 2 cm^{-1}.

2.2.2.2. Computational details. The intra- and inter- molecular interactions between the CMC and PVA were studied via density functional theory (DFT) calculations which executed by Gaussian G09 W software. The simulation was performed based on gradient corrected DFT [21] using the Becke three-parameter hybrid functional (B3) [22] which is for exchange component and the Lee-Yang-Parr (LYP) correlation function [23]. Chemical structures of pure CMC, PVA, and CMC/PVA complexes were built and arranged based on their internal coordinates (bond length, bond angle, and dihedral angle) using GaussView 5.0 software. The internal coordinates of the models were then optimized to the lowest energy structure using B3LYP

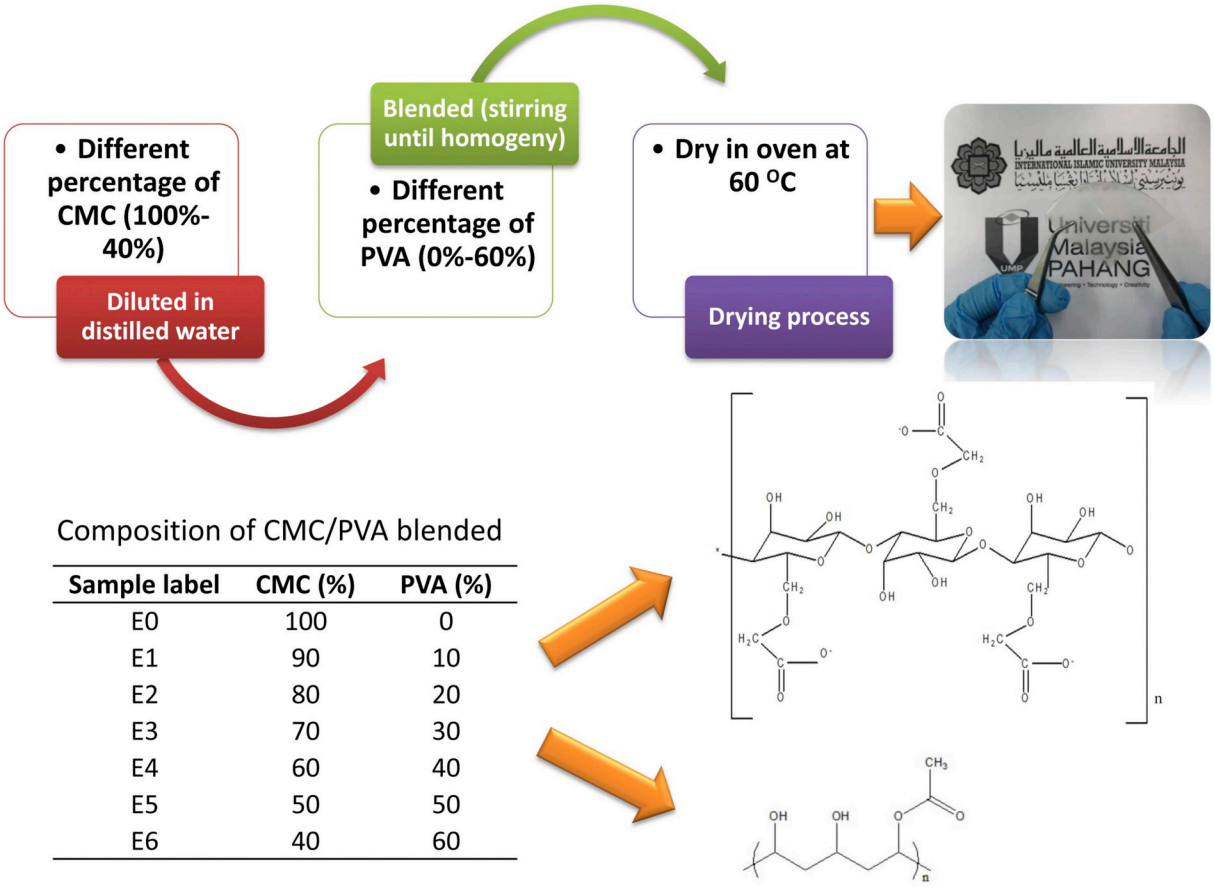

Fig. 1. Schematic preparation, thin film appearance and blended composition.

functional and 6-31 g (d, p) basis set [24]. The modeled structures were then examined using the harmonic frequency calculations using the same functional and basis set. The calculated mode of vibration of the optimized structures presented positive frequencies, which indicate minimum energy structures [23]; evaluated as realistic models. The stage of validation and establishment of the realistic models is crucial; would yield trustworthy information to be compared with that of the experimental observations.

2.2.3. X-ray diffraction (XRD)

XRD analysis is useful tool in the determination of degree of crystallinity and amorphousness. The XRD measurements were performed using XRD-Rigaku MiniFlex II outfitted with nickel-filtered C_u K_α ($\lambda = 0.154$ nm) radiation (30 kV, 15 mA) and scanned at angle 2θ between 5° to 80°. Meanwhile, the XRD deconvolution analysis was performed using Origin Lab 8.0 software in order to deconvolute specific region (crystal or amorphous peaks). The crystalline and amorphous peaks were deconvolute based on the assumption of Gaussian function in order to ensure all peaks are fit with original spectrum. The percentage of crystallinity was determined by using Eq. (1) [25] as follows:

$$X_c = \frac{A_c}{A_T} \times 100\% \quad (1)$$

where A_c is an area of crystalline region, A_a is an area of amorphous region, A_T is the total area under the peak representing the area of crystalline region and area of amorphous region and X_c is the degree of crystalline in percentage.

Further analysis on the crystallite size (D) was done using full width at half maximum (FWHM) information. The calculation is based on Debye-Scherrer equation shown in Eq. (2).

$$D = \frac{K\lambda}{FWHM \cos\theta} \quad (2)$$

where K is 0.94, λ is the X-ray wavelength used which is 0.154 nm and θ is the peak location.

2.2.4. Differential scanning calorimetry (DSC)

Thermal properties such as glass transition temperature, melting temperature and crystallization temperature can be measured by using DSC. The thermal properties of the HPe system are determined by DSC analysis which was conducted using DSC TA Q500 model where the electrolyte was sealed in a pan of aluminum. An empty pan was used as reference. The HPe system was heated at an elevated temperature to erase previous thermal history, and then cooled at a linear rate before heating again. The glass transition temperature (T_g) of HPe system was analyzed using TA Universal analysis at a heating rate of 10 °C min^{-1} from 37 to 300 °C. A nitrogen flow (50 mL min^{-1}) was applied during the experiment.

2.2.5. Thermogravimetric analysis (TGA)

Mettle Toledo TGA-DSC was operated from 30 to 800 °C at a heating rate of 10 °C min^{-1} to analyze ~3 mg of HPe sample sealed into aluminum oxide pan for TGA analysis.

2.2.6. Electrical impedance spectroscopy (EIS)

The conductivity measurement was carried out using 3532–50 LCR Hi-TESTER (HIOKI) and been tested at ambient temperature at frequency ranges between 50 Hz to 1 MHz. The HPe thin film was sandwiched in between blocking electrodes made of stainless steel. The conductivity is calculated using the following equation:

$$\sigma = \frac{t}{R_b A} \quad (3)$$

where t is the thickness of the fiilm, A is the area of contact surface and R_b represents the bulk resistance.

3. Results and discussions

3.1. SEM analysis

SEM images for various composition of CMC/PVA are compared in Fig. 2. The SEM elucidates the surface morphology of the HPe system at 25 μm resolution and indicates a continuous microstructure of the blend

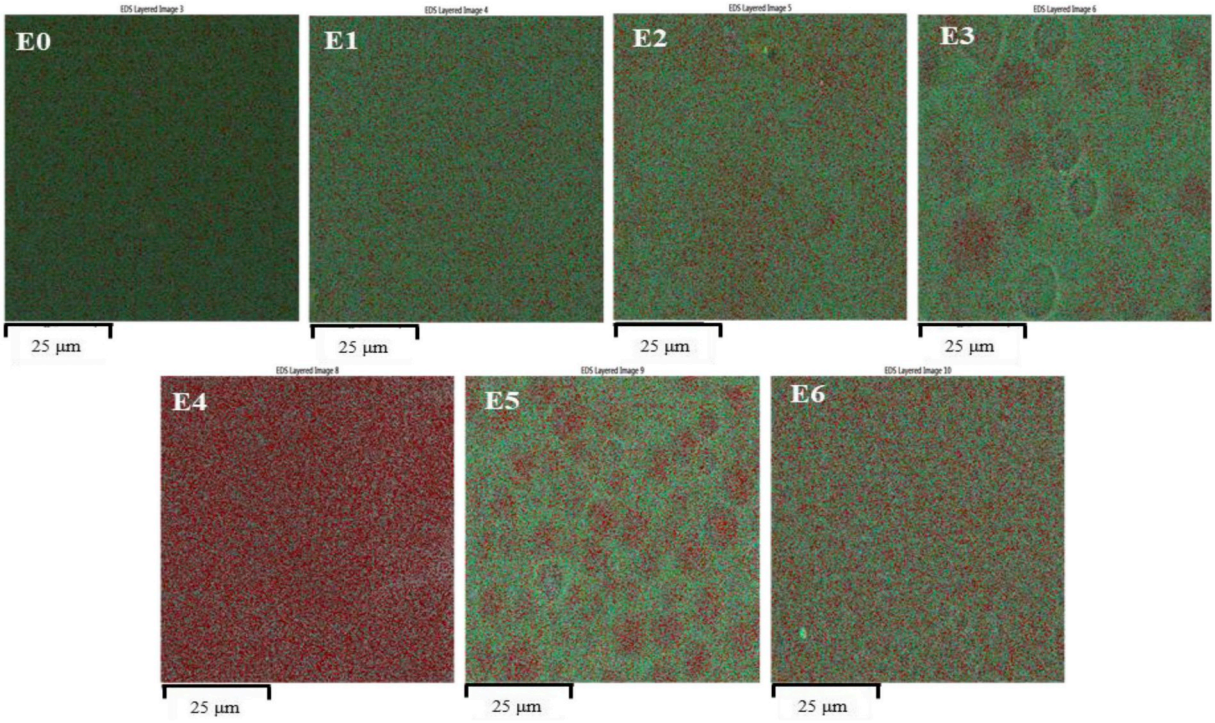

Fig. 2. SEM microphotography at resolution 25 μm for various HPe system.

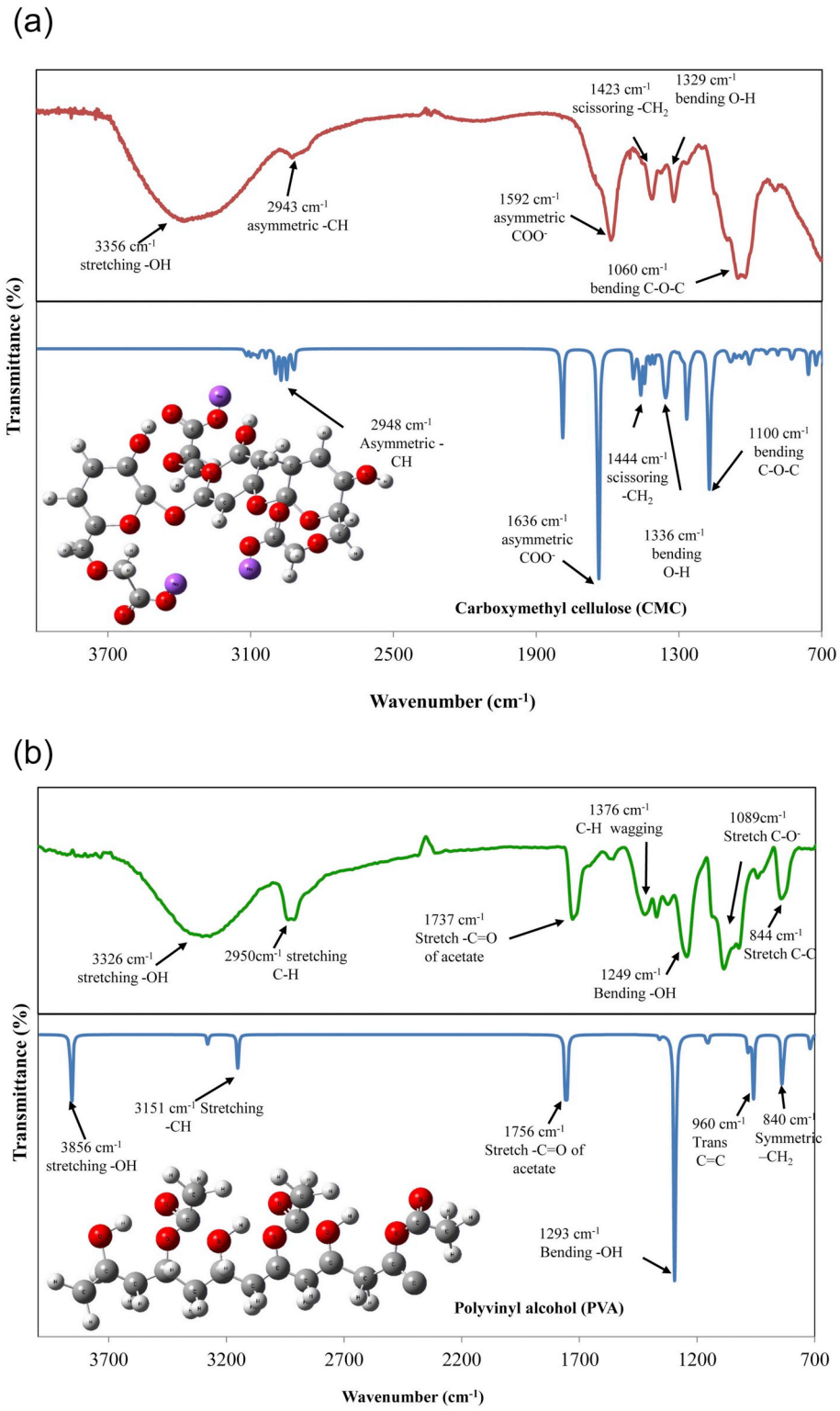

Fig. 3. Experimental FTIR spectra (top) and calculated spectra (bottom) of (a) pure CMC and (b) pure PVA of the HPe system. Inset shows the optimized structure of the CMC and PVA.

system with no phase segregation in this resolution which suggests the amorphous nature. These results corroborate the findings of Fasihi et al. [26], who suggested that HPe system has a good miscibility ascribed to the H-bonding formed between CMC and PVA. Apparently, the micrographs show that additional of PVA creates some regular globules with various sizes, beyond sample E2 throughout the system suggesting that size of globules depending on the blend ratio of the HPe system [27].

3.2. IR spectroscopy

The prominence of IR spectroscopy is to characterize the configuration and conformation structure of polymers to explain the complexation between the bio-polymer blends. The most common complexation in polymer is the hydrogen bonding (H-bonding) which become literally important to change the crystallinity nature of wide

Table 1
List of ATR-FTIR vibrational modes of CMC and PVA.

Sample	Wavenumber (cm^{-1})	Assignment	References
Carboxymethyl cellulose (CMC)	1060	Bending C−O−C	[34]
		Ether linkage or 1,4-beta-d glucoside	[35]
	1329	Bending −OH	[36]
	1423	Scissoring $-CH_2$	[36,37]
	1592	Asymmetrical COO^-	[36,38,39]
	2943	Aliphatic −CH	[35,38]
	3356	Stretching −OH	[36,38]
Polyvinyl alcohol (PVA)	844	Stretch C−C	[34]
	1089	Stretching $C-O^-$	[34]
	1246–1376	Peaks correspond to motion of the carbon skeleton	[35]
	1376	Wagging −CH	[40]
	1737	Stretching C═O and C−O from acetate group remaining from PVA	[35,41]
	2950	Stretching −CH	[33]
	3326	Stretching −OH	[34,35]

range materials. Meanwhile, the calculated IR spectra of CMC and PVA and optimized structure for both compounds are compared with the experimental ATR-FTIR spectra and presented in Fig. 3(a) and (b) respectively; showed similar peak positions with minimal differences. The ATR-FTIR data for CMC and PVA is tabulated in Table 1. There are five absorption bands which appeared in the region 1060 cm^{-1}, 1329 cm^{-1}, 1423 cm^{-1}, 1592 cm^{-1} and 3356 cm^{-1} correspond to bending C−O−C, bending −OH, scissoring $-CH_2$, asymmetric $-COO^-$ and stretching −OH respectively which are considered as the signature peaks of the CMC. Samsudin et al. [12] reported the similar signature bands of the CMC at 1056 cm^{-1}, 1334 cm^{-1}, 1421 cm^{-1} and 1581 cm^{-1}. These are the characteristic peaks of carbohydrate and confirmed the carboxymethyl substituent at the CMC backbone. The pure PVA showed absorption bands at 844 cm^{-1}, 1089 cm^{-1}, 1376 cm^{-1}, 1737 cm^{-1} and 3326 cm^{-1}, attributed to the stretching C−C, stretching $-CO^-$, wagging −CH, stretching C═O and stretching −OH respectively. The main features of PVA given by the appearance of vibration carbon skeleton motion at the range 1089 to 1376 cm^{-1}

The ability to simulate realistic cluster models is a key point to produce significant results of theoretical calculations [28]. The DFT calculations could provide structural information of a set of molecule such as polymer with a relatively higher precision of 1–2% [29]. According to Scott and Radom, [30], the DFT able to provide important prediction concerning on the vibrational frequencies of a broad range of molecules with percentage of accuracy of 5–10% which can eventually correlate the ATR-FTIR characterization of the HPe system in this present work. The vibrational frequency of CMC and PVA were determined using single scaling factor, 0.95 [31]. It is worthy to note that the wavenumber measured by the DFT analysis of CMC, PVA and CMC/PVA HPe system are about the same with the ATR-FTIR analysis. This work supports the observations made by previous studies [28,31–33]. The result explicates that DFT calculations may give significant input for comparative studies and the results obtained reflect the overall trend which was observed in FTIR analysis.

Riaz et al. [42] mentioned that the physical properties of polymer blend are influenced by the molecular chain of the polymer. The study on the complexation of the polymer blend electrolyte process can be explained through different types of interaction such as H-bonding and configuration which help to predict the thermal and electrical properties of the HPe system [43,44]. H-bonding interaction is well known with its diversity and strength [45]. Xing et al. [46] reported that polymers contain the hydroxyl group can be mixed with polyester because of the intermolecular H-bonding resulting in completely or partially miscible system. Meanwhile in this present work, the peak intensity of the C−O−C, −COO− and −OH found at 1060 cm^{-1}, 1329 cm^{-1}, 1592 cm^{-1} and 3356 cm^{-1} has reduced in comparison to other peaks suggesting the occurrence of intermolecular H-bonding during the complexation in the hybrid polymer system. A study conducted by Coleman et al. [47] revealed that the process to hybrid two polymers require favorable interaction at active sites such as oxygen and nitrogen which has capability to exert strong forces of attraction (H-bonding). The evaluation of the complexation between CMC and PVA HPe is done based on changes to position, shift in absorption and change in peak intensity attributed to the disappearance/appearance of peak at specific region [48]. The finding for the theoretical spectra of the CMC blend with PVA presented in Fig. 4 shows a similarity in terms of vibrational frequency and modes as reported by previous researchers via experimental works [35,36,40,41].

The ATR-FTIR spectrum is analyzed based on three potential regions in Fig. 5 which are at the following wavenumber (a) 800 to 1200 cm^{-1} (b) 1200–1800 cm^{-1} and (c) 2700 to 3500 cm^{-1} in order to have more apparent evaluation. Fig. 5(a) reveals the complexation for hybrid polymer with dual polymer host of CMC and PVA. The most intensive spectrum is found at 1060 cm^{-1} due to ether linkage (C−O−C) which does contain the oxygen site that is capable to form the inter-molecular H-bonding with another molecule such as PVA [47]. This is supported by an obvious shifting to higher wavenumber, 1060 cm^{-1} to 1098 cm^{-1} and thus, confirmed the interaction between CMC and PVA. Two bands located at 1329 cm^{-1} and 1592 cm^{-1} shown in Fig. 5(b) correspond to intramolecular forces of the hydroxyl and carboxylate group. Band intensity for both peaks are gradually decreased until E2 and eventually disappear when content of PVA exceeds the 20 percentage composition. The intermolecular forces of H-bonding predominated between the CMC and PVA of the HPe system, where the formation are expected to take place at the region assigned to the bending −OH and asymmetric $-COO^-$ functional group as they are the major indicative bands for the complexation [29]. El sawy et al. [34] has also discovered the complexation to occur within these two regions. Apparently, the absorption band of bending –OH of CMC has shifted from wavenumber 1329 cm^{-1} to 1354 cm^{-1} confirmed the complexation between CMC and PVA.

Beyond sample E3 the peak at wavenumber 1329 cm^{-1} and 1423 cm^{-1} begin to be substituted by wagging −CH of PVA. Another obvious complexation which appears at 1592 cm^{-1} assigned to free carboxylate anion ($-COO^-$) and shifted to 1598 cm^{-1}ascribed by H-bonded carboxylate ($-COO^-$) [49]. We can speculate that the optimum number of hydrogen bond between CMC and PVA has occurred until E2 sample since the pattern was observed from sample E0 until E2 [50]. Conversely, this carboxylate peaks disappeared when PVA was added progressively beginning from E3 until E6 suggesting the substitution of PVA into the CMC [25]. The appearance of new peak corresponds to C═O stretching at 1740 cm^{-1} was attributable to PVA used in this work which is partially hydrolyzed (~85%). Thus, the carbonyl band was expected to appear around that region [20,51]. Fig. 5(c) represents a broad absorption band at the region 3356 cm^{-1} corresponds to free hydroxyl group of CMC. The addition of PVA leads to the formation of

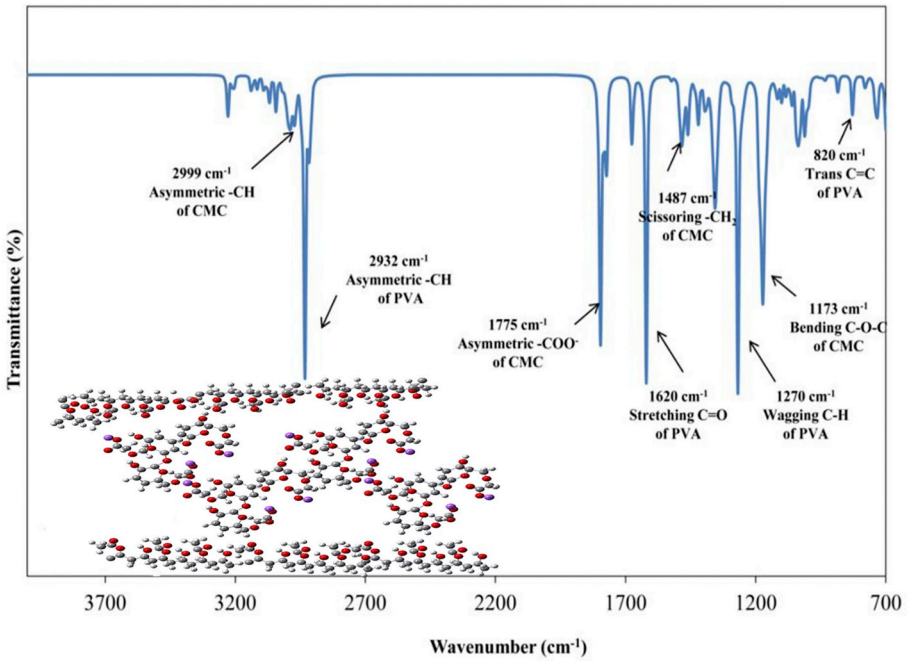

Fig. 4. Theoretical FTIR spectra of CMC hybrid with PVA. Inset shows the optimized structure of the CMC-PVA HPe system.

hydrogen-bonded hydroxyl groups in the HPe system and causes the band getting narrow and shifted to lower wavenumber, 3326 cm^{-1}. There is a small hump observed at 2943 cm^{-1} due to stretching −CH which experience a shifting to higher wavenumber, 2954 cm^{-1}.

Based on Fig. 5(a) and (b), two new shoulder peaks start to appear for E2 sample at 844 cm^{-1} and 1737 cm^{-1} which is referring to vibration of stretching C−C and C═O of PVA with increasing PVA content. The transmittance of the shoulder peak has increased compare to that of the original band with increasing PVA content which gives reflection that complexation has occurred. Based on the analysis, sample E2 showed significant changes through blending method. This explain that composition of 80:20, CMC/PVA HPe system has been complexed with the finest interaction due to the appearance of new peak while retaining the original features of polymers used in this work. This is expected would lead to improve in the amorphousness and thermal stability of the sample. However, this hypothesis requires further investigation in order to achieve a parallel explanation.

3.3. XRD analysis

Fig. 6(a) shows the XRD spectrum of pure CMC and pure PVA at ambient room temperature from 2° to 80°. Three diffraction peaks for the pure CMC appeared at 2θ, 20.7°, 34.4° and 44.7°. On the other hand, pure PVA has two sharp diffraction peaks at 19.9° and 34.7° correspond

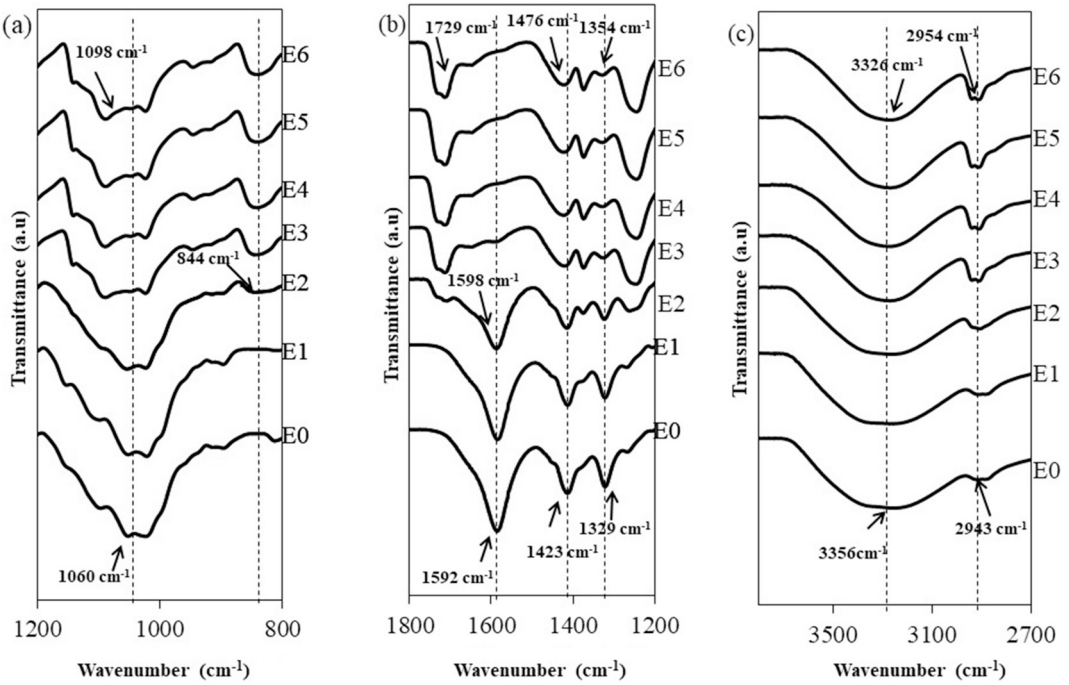

Fig. 5. FTIR spectrum for CMC/PVA of HPe system in the wavenumbers of (a) 800–1200 cm^{-1}, (b) 1200–1800 cm^{-1} and (b) 2700–3500 cm^{-1}.

to an orthorhombic lattice (110) reflection [52]. The two polymers applied in this study is generally semi-crystalline materials because of the occurrence both crystalline and amorphous region [53–55]. However, based on the analysis, the change in amorphousness of CMC can be seen after the introduction of PVA into the CMC as the diffraction peak becomes less intense. It can be inferred that complexation has taken place between CMC and PVA. On top of that, crystalline peaks correspond to PVA was not present in the sample up to E2 sample and indicating complete dissociation or success of miscibility which suggests greater diffusion and conductance ability [56].Thus, blending method revealed the success in terms of miscibility and compatibility within the polymer blend based on the change in the intensity and area under the peaks which becomes broadened [57] (see Table 2).

As discussed in FTIR analysis, the carboxylate anion of CMC has interacted with hydroxyl group of PVA resulting in ion-dipolar complexes which can lessen the polymer chain rigidity and hence decreasing the degree of crystallinity [58]. The complexation in CMC/PVA HPe system was expected to occur via intra- or inter-chain hopping between polar functional group of the two host polymer. Consequently, the polymer chain become lack in orderly structure and become more amorphous which could facilitate for higher conductivity. However, the crystallinity of the blend polymer was increased progressively with an increase amount of PVA from E3 until E6 samples which influenced by the nature of PVA since it is more crystalline and affect the interaction between the CMC and PVA.

Fig. 6(b) presents the XRD deconvolution for HPe system. Based on the calculated value; sample E2 gives the lowest percentage of crystallinity (more amorphous) which is 16.02%. The extension study of crystallite size was done using the information of full width half maximum (FWHM) and calculated by using Scherrer equation which further supports the nature of the HPe system studied in this work. The calculated value of crystallite size shown a value of 16.80 ± 0.06 Å, 8.24 ± 0.06 Å, 7.37 ± 0.06 Å and 38.21 ± 0.06 Å for sample E0, E1, E2 and E3, respectively. The incorporation of PVA managed to alter the crystallite size of the HPe system. The calculated value obtained from the deconvolution was in line with the Debye Scherrer relation where the lowest percentage of crystallinity sample possesses the smallest crystallite size which is shown by E2 sample. The increased in amorphous region in the polymer electrolyte ascribed by delocalized complex system that affects the flexibility of the CMC backbone [59]. Nonetheless, it is obvious that the intensity of E3 increases as more PVA added suggesting that E3 until E6 sample possessed higher degree of crystallinity and larger crystallite size. However, the deconvolution technique offers semi-quantitative evaluation for the amount of crystalline and amorphous of the HPe system which is useful for comparison with experimental result in the XRD analysis [60,61].

3.4. Thermal analysis

Thermogram of DSC shows heating run for various composition CMC/PVA HPe system up to 300 °C and presented in Fig. 7. Based on the thermogram, there are two endothermic peaks observed which correspond to glass transition and melting phase transition. The information on physical parameters of glass transition temperature (T_g) explain the degree of purity and nature of the substance [62]. The glass and melting temperature of the HPe system is listed in Table 3. Obviously, thermal transition of CMC varied after the incorporation of PVA at different composition. Broad endothermic peaks around 47 to 73 °C and 170 to 184 °C is referring to T_g and T_m of semi-crystalline [15]. These observations signify the compatibility between the CMC and PVA which is mainly due to the characteristic of hydroxyl and carboxylate anion group that facilitate the interaction via H-bonding and the result also shows agreement with other report [15,63,64]. According to Andreev et al. [65], T_g is crucial in determining the characteristic of polymer chain in terms of segmental motion that enhance the conductivity. The value of T_g decreases to the lowest temperature of 47.4 °C with enthalpy, ΔH of 174 J/g for E2 samples suggesting that the flexibility increases in the CMC/PVA HPe system chain. This suggests the present sample E2 is suitable to act as host polymer in the further expansion of polymer electrolytes system. However, upon the addition of more PVA, the T_g increases as the H-bonding interaction between CMC and PVA become stronger. This result is also in accordance with Ying et al. [66] which states that H-bonding and T_g is directly related in qualitatively. However, the value of T_g observed for sample E3 and E6 is not quite consistent with the percentage of crystallinity discussed in XRD previously. At higher composition of PVA, optimum number of intermolecular hydrogen bonding leading to more disturbance in the order of PVA molecular chains and creating some free volumes. In 2010, Napolitano et al. [67] pointed to some of the ways in which the presence of free volume could further contribute in the reduction of T_g. This finding corroborates with those of other studies who worked on hybrid system of polymer which discovered similar inconsistent trend where the discrepancy might be attributed to the interaction between two polymers via inter-molecular H-bonding that could lead to stiffening molecular chain and hence affecting the thermal transition to lower value for sample E6 in comparison to sample [68–70].

TGA thermogram of CMC/PVA HPe system is shown in Fig. 8 and the inset was referring to thermogram of pure CMC. The curves elucidate thermal stability of the HPe system which the degradation has completed in three stages. TGA curve of E1 and E2 showed similar pattern to that of pure CMC and had a slower slope. Based on pure CMC curve, the first stage in the range of 25 to 200 °C is associated to loss of water. This first decomposition involved a small weight loss (10–15%) which is due to the decomposition of hydroxyl group. This result was in agreement with study performed by El Sayed et al. [15] Pure CMC is hygroscopic (high moisture sensitivity), blending CMC with other polymer able to improve this problem which is clearly shown at the first region.

The second decomposition showed more significant weight loss in the temperature range 250 to 325 °C. This decrease is because of the degradation of the characteristic structure of CMC which is the carboxylate group that occupies about 20% of each HPe system [71]. TGA curve of E0 until E2 showed a slower slope demonstrating high thermal stability whereas E3 until E6 HPe system experience a rapid weight loss which become unfavorable in polymer electrolyte system because of low thermal stability. According to Mahdavinia et al. [72] the decomposition of bond scission in PVA backbone can be found in the range of 318 to 450 °C. Obvious gap in the weight loss has been monitored at

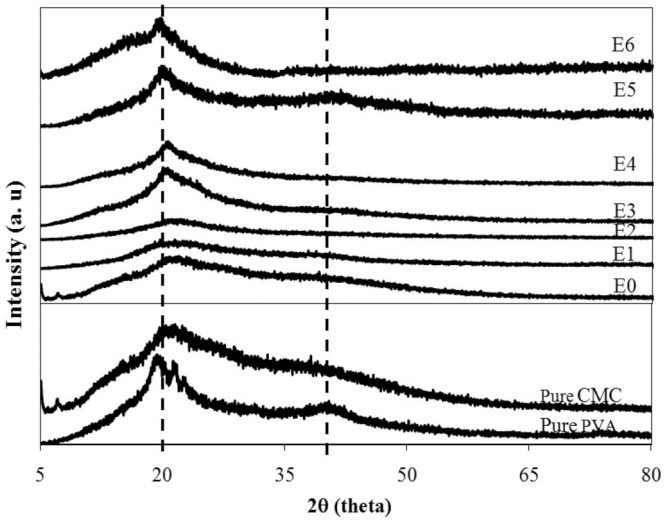

Fig. 6. XRD analysis (a) Experimental XRD spectrum and (b) Fitting XRD deconvolution for pure CMC, pure PVA and CMC/PVA HPe system.

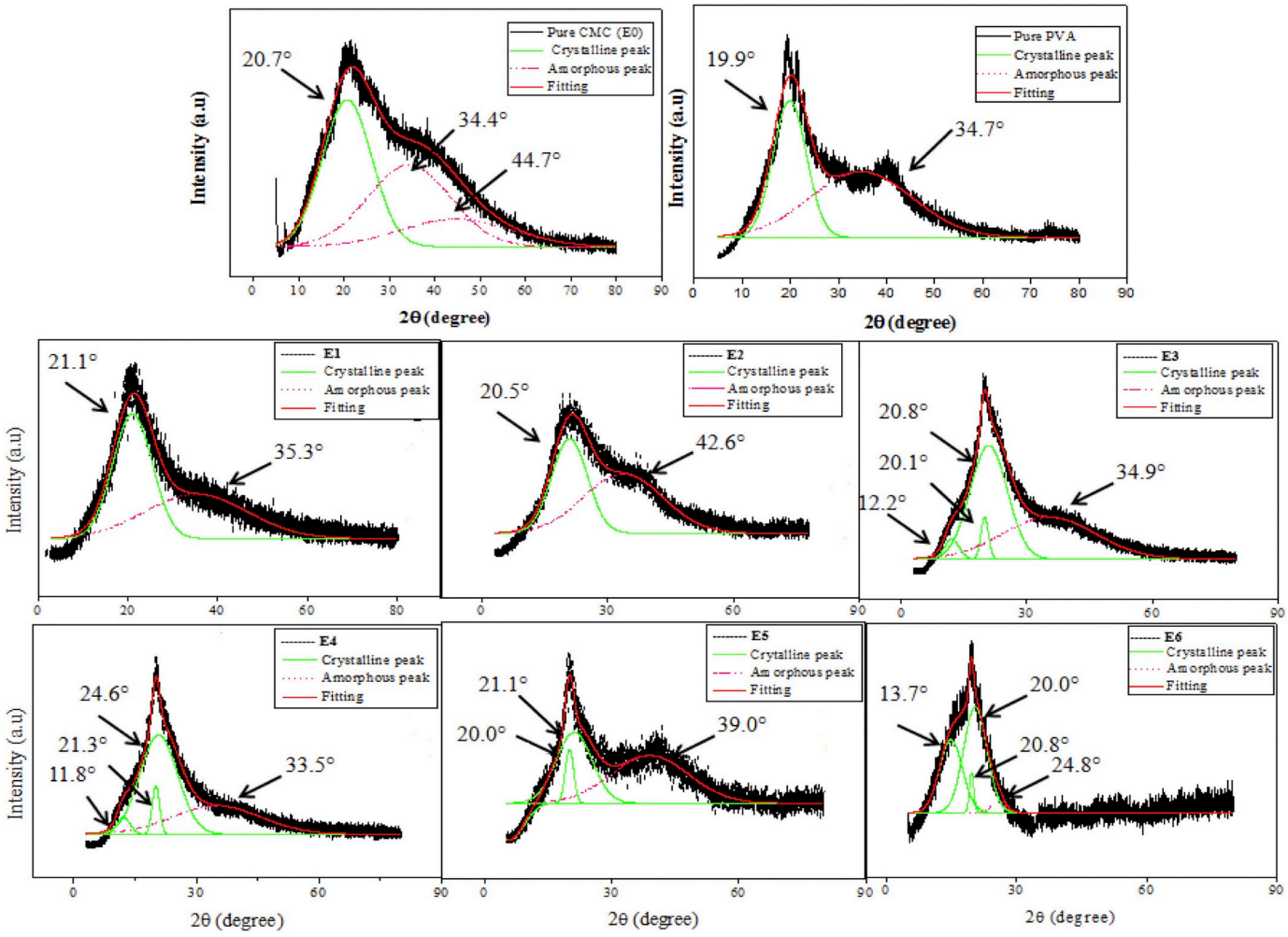

Fig. 6. (*continued*)

this region which is an indication of lower thermal stability with increasing PVA content. The observation reveals that at higher temperature, the disruption of H-bonding in the HPe system has happened for the system containing more than 20 weight percentage [73].

It was noted the final stage which is the plateau region was due to the decomposition of the remaining carbonaceous material and ash formation [74]. The weight loss of E0, E1 and E2 occurred with slower slope and more plateau compared to E3 until E6 again confirming the thermal stability of HPe system with less than 20 weight percentage of PVA. Table 4 shows the maximum decomposition temperature (T_d) for all HPe system study in this work. The data revealed that E2 sample showed the least weight loss could be attributed to the enhancement of interaction and amorphous phase of the CMC/PVA as explained by FTIR and XRD analysis and led to enhance the thermal stability. Based on the observations, it shows the present sample is a promising to be act as polymer host in electrolyte system where can stand at higher temperature above 90 °C [20].

Table 2
Percentage of crystallinity of CMC/PVA HPe system.

Sample	A_c	A_a	X_c (%)
E0	5248.78	7091.87	42.53
E1	5690.20	25,532.73	18.22
E2	7044.07	36,940.58	16.015
E3	5580.90	4517.37	55.27
E4	4202.45	2420.32	63.45
E5	2642.87	1492.55	63.91
E6	1560.67	217.53	87.77

3.5. Conductivity analysis

Conductivity measurement is conducted in order to reveal the effect of HPe system by addition of PVA into the CMC. Based on the previous analysis, the crystallinity of the HPe system has reduced upon the incorporation of the PVA which was proven by the XRD analysis. In

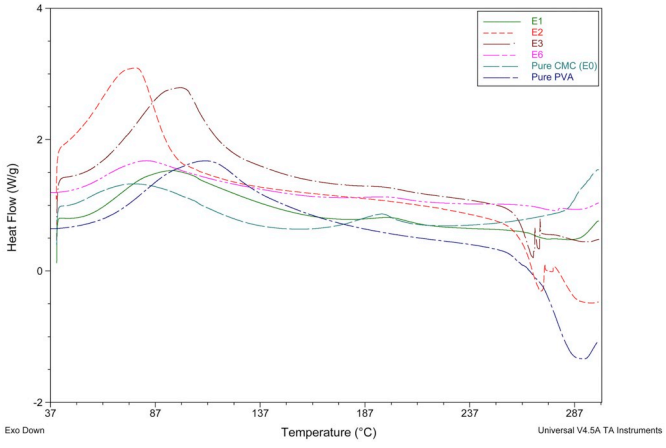

Fig. 7. DSC thermogram for various composition CMC/PVA HPe system.

Table 3
Glass and melting phase transition of CMC/PVA HPe system.

Sample	Glass phase transition		Melting phase transition	
	T_g (°C)	ΔH (J/g)	T_m (°C)	ΔH (J/g)
Pure CMC (E0)	55.3	62	173	23.1
Pure PVA	89.7	374	–	–
E1	71.6	236	182	9.12
E2	47.4	174	–	–
E3	73.2	362	181	2.27
E6	60.8	215	184	3.48

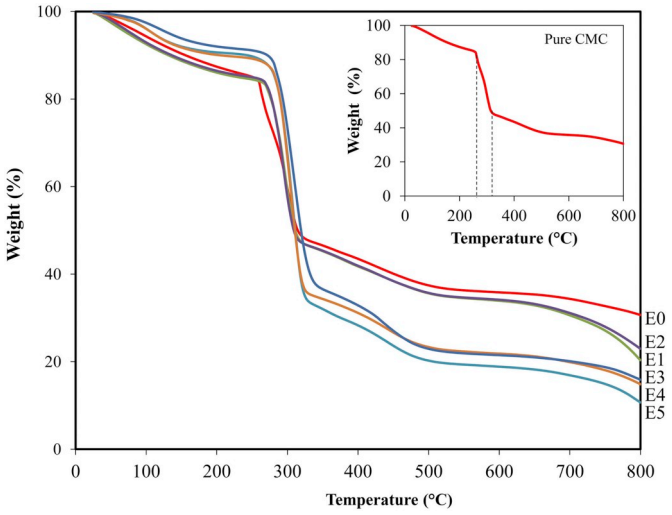

Fig. 8. TGA thermogram of various CMC/PVA HPe system.

conjunction to these results, the conductivity of the HPe system was further investigated. The conductivity values of HPe system are illustrated in Fig. 9 and showed the increasing of conductivity when CMC blended with PVA. The plot shows that sample E2, with composition of 80:20 is the optimum composition for this present work with conductivity ta room temperature is $(9.12 \pm 0.04) \times 10^{-6}$ S/cm. This increment was due to higher amorphous phase and lowest weight loss which was confirmed from XRD and TGA analysis.

PVA is well known with its chain flexibility allowing random intra- and inter- molecular attraction forces between the host polymers which can promote the segmental motion which can increase the chain mobility and hence increasing the conductivity [75]. This is supported by the XRD analysis where crystallinity phase has decreased until sample E2 and hence increasing the conductivity. Rajeh et al. [76] in his study about the enhancement of spectroscopic and electrical properties of polyethylene oxide/carboxymethyl cellulose blends revealed the increase in amorphous of polymer blend could increase the electrical conductivity. This result also supported by DSC where T_g becomes lower and fasten the chain mobility and hence increasing the

Table 4
Maximum decomposition temperature of various composition CMC/PVA HPe system.

Sample	Maximum decomposition temperature, T_d (°C)	Weight loss (%)
E0	311.16	48.40
E1	306.83	47.16
E2	305.00	47.09
E3	309.83	50.67
E4	316.67	58.43
E5	318.33	59.82
E6	327.33	57.24

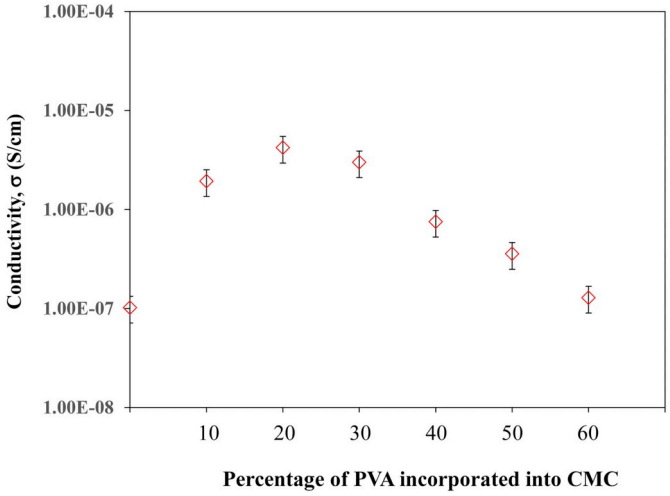

Fig. 9. Variation plot of conductivity as a function of percentage of PVA incorporate into CMC.

conductivity. It can be seen that upon the addition of PVA above 20% in CMC, the conductivity starts to decrease to a lower value. This can be due to reappearance of crystal peak where huge amount of PVA can trigger the improvement in crystallization of HPe system [77]. Furthermore, excess amount of PVA causes rapid weight loss due to the weak interaction between the CMC and PVA as revealed by FTIR and TGA.

Table 5 provides a comparison of conductivity for single polymer and polymer blend system. The finding reveals that CMC/PVA HPe system possessed relatively higher conductivity as compared to single polymer and also polymer blend as electrolyte systems. Therefore, this present system conveys that the CMC/PVA HPe system is a promising candidate to act as a host for polymer electrolytes system in electrochemical applications. [19,78–81]

4. Conclusion

Hybrid polymer (HPe) system based carboxymethyl cellulose (CMC) complexed with polyvinyl alcohol (PVA) was successfully prepared via solution casting method. The complexation between CMC and PVA were found at 1060 cm^{-1}, 1329 cm^{-1}, 1592 cm^{-1}, and 3356 cm^{-1} $^{-1}$ correspond to bending C—O—C, bending —OH, asymmetric —COO^- and stretching —OH respectively based on FTIR analysis. The calculated IR spectra showed good agreement with the experimental IR spectra, thus confirming the interaction in CMC/PVA via H-bonding. The XRD and deconvolution shows a gradual decrease in peak intensity upon addition of 20% PVA due to an increase in the amorphous nature of the HPe. This revealed the intermolecular H-bonding drives the reduction in degree of crystallinity. The TGA and DSC thermogram evidenced good thermal stability and miscibility were observed for sample 80:20. T_g for the 80:20 composition of HPE was found to be the lowest indicating amorphousness predominate and weaker H-bonding forces. The blend

Table 5
Comparison of conductivity for single and hybrid polymer from the literatures.

Polymer host	Conductivity, σ (S/cm)	Reference
Kappa-carrageenan	~10^{-8}	[25]
CMC	~10^{-8}	[78]
PVA	~10^{-7}	[79]
Sago starch	~10^{-7}	[80]
CMC/Chitosan	~10^{-8}	[81]
Starch/Chitosan	~10^{-9}	[17]
Chitosan/PVA	~10^{-7}	[20]
CMC/PVA	~10^{-6}	Present system

of 80:20 compositions of CMC/PVA hybrid polymer (HPe) system was found to be the optimum ratio with higher conductivity of $(9.12 \pm 0.04) \times 10^{-6}$ S/cm. The influence of hybrid composition in enhancing the conductivity of CMC/PVA HPe system has been proved via impedance spectroscopy. Together these results show a preference for further modification such as addition of appropriate ionic dopant which can further increase the degree of amorphousness and hence increasing the electrochemical property of the HPe system.

Acknowledgement

The authors would like to thank MOHE for FRGS (RDU170115), Faculty of Industrial Sciences & Technology, Universiti Malaysia Pahang, and Japan Advanced Institute of Science and Technology (JAIST) for the help and support given for the completion of this work.

References

[1] D. Fenton, J. Parker, P. Wright, Complexes of alkali metal ions with poly (ethylene oxide), Polymer 14 (1973) 589.
[2] B. Scrosati, Recent advances in lithium ion battery materials, Electrochim. Acta 45 (2000) 2461–2466.
[3] M. Li, X. Wang, Y. Yang, Z. Chang, Y. Wu, R. Holze, A dense cellulose-based membrane as a renewable host for gel polymer electrolyte of lithium ion batteries, J. Membr. Sci. 476 (2015) 112–118.
[4] M. Shukur, R. Ithnin, H. Illias, M. Kadir, Proton conducting polymer electrolyte based on plasticized chitosan–PEO blend and application in electrochemical devices, Opt. Mater. 35 (2013) 1834–1841.
[5] M. Buraidah, L. Teo, S. Majid, R. Yahya, R. Taha, A. Arof, Characterizations of chitosan-based polymer electrolyte photovoltaic cells, Int. J. Photoenergy 2010 (2010).
[6] S. Rudhziah, A. Ahmad, I. Ahmad, N. Mohamed, Biopolymer electrolytes based on blend of kappa-carrageenan and cellulose derivatives for potential application in dye sensitized solar cell, Electrochim. Acta 175 (2015) 162–168.
[7] F. Bella, N.N. Mobarak, F.N. Jumaah, A. Ahmad, From seaweeds to biopolymeric electrolytes for third generation solar cells: an intriguing approach, Electrochim. Acta 151 (2015) 306–311.
[8] M. Fujishima, H. Takatori, K. Yamai, Y. Nagao, H. Kitagawa, K. Uchida, Proton conductivity of biopolymer–platinum nanoparticle composite under high humidity, J. Mater. Sci. 43 (2008) 3130–3134.
[9] C. Tan, A. Ahmad, F. Anuar, Synthesis and characterization of polylactide-poly (ethylene glycol) block copolymer as solid polymer electrolyte, Asian J. Chem. 26 (2014).
[10] H.-L. Hsu, C.-F. Tien, Y.-T. Yang, J. Leu, Dye-sensitized solar cells based on agarose gel electrolytes using allylimidazolium iodides and environmentally benign solvents, Electrochim. Acta 91 (2013) 208–213.
[11] R. Singh, N.A. Jadhav, S. Majumder, B. Bhattacharya, P.K. Singh, Novel biopolymer gel electrolyte for dye-sensitized solar cell application, Carbohydr. Polym. 91 (2013) 682–685.
[12] A. Samsudin, M. Isa, Structural and ionic transport study on CMC doped NH_4Br: a new types of biopolymer electrolytes, J. Appl. Sci. 12 (2012) 174–179.
[13] K.M. El Salmawi, Application of polyvinyl alcohol (PVA)/carboxymethyl cellulose (CMC) hydrogel produced by conventional crosslinking or by freezing and thawing, J. Macromol. Sci. A 44 (2007) 619–624.
[14] M. Shukur, M. Kadir, Hydrogen ion conducting starch-chitosan blend based electrolyte for application in electrochemical devices, Electrochim. Acta 158 (2015) 152–165.
[15] S. El-Sayed, K. Mahmoud, A. Fatah, A. Hassen, DSC, TGA and dielectric properties of carboxymethyl cellulose/polyvinyl alcohol blends, Phys. B Condens. Matter 406 (2011) 4068–4076.
[16] L.A. Utracki, C.A. Wilkie, Polymer Blends Handbook, Springer, 2002.
[17] A. Khiar, A. Arof, Electrical properties of starch/chitosan-NH_4NO_3 polymer electrolyte, WASET 59 (2011) 23–27.
[18] M.S.A. Rani, N. Mohamed, M.I.N. Isa, Characterization of Proton Conducting Carboxymethyl Cellulose/Chitosan Dual-Blend Based Biopolymer Electrolytes, Materials Science Forum, Trans Tech Publications Ltd., 2016, p. 539.
[19] P. Joge, D.K. Kanchan, P. Sharma, N. Gondaliya, Effect of nano-filler on electrical properties of PVA-PEO blend polymer electrolyte, Indian J. Pure App. Phys. 51 (2013) 350–353.
[20] M. Buraidah, A. Arof, Characterization of chitosan/PVA blended electrolyte doped with NH_4I, J. Non-Cryst. Solids 357 (2011) 3261–3266.
[21] P. Hohenberg, W. Kohn, Inhomogeneous electron gas, Phys. Rev. 136 (1964) B864.
[22] A.D. Becke, Density-functional thermochemistry. III. The role of exact exchange, J. Chem. Phys. 98 (1993) 5648–5652.
[23] C. Lee, W. Yang, R.G. Parr, Development of the Colle-Salvetti correlation-energy formula into a functional of the electron density, Phys. Rev. B 37 (1988) 785.
[24] X. Wang, C. Wang, H. Zhao, Errors in the calculation of 27Al nuclear magnetic resonance chemical shifts, Int. J. Mol. Sci. 13 (2012) 15420–15446.
[25] N. Zainuddin, A. Samsudin, Investigation on the effect of NH_4Br at transport properties in K–carrageenan based biopolymer electrolytes via structural and electrical analysis, Mater. Today Commun. 14 (2018) 199–209.
[26] H. Fasihi, M. Fazilati, M. Hashemi, N. Noshirvani, Novel carboxymethyl cellulose-polyvinyl alcohol blend films stabilized by Pickering emulsion incorporation method, Carbohydr. Polym. 167 (2017) 79–89.
[27] A. Adegbola, I.E.A. Aghachi, O. Sadiku-Agboola, SEM and AFM microscopical characterization of rPAN fibre and PET blends, Alexandria Eng. J. 57 (2018) 475–481.
[28] M. Orio, D.A. Pantazis, F. Neese, Density functional theory, Photosynth. Res. 102 (2009) 443–453.
[29] J.C. Cuevas, J. Heurich, F. Pauly, W. Wenzel, G. Schön, Theoretical description of the electrical conduction in atomic and molecular junctions, Nanotechnology 14 (2003) R29.
[30] A.P. Scott, L. Radom, Harmonic vibrational frequencies: an evaluation of Hartree − Fock, Møller − Plesset, quadratic configuration interaction, density functional theory, and semiempirical scale factors, J. Phys. Chem. 100 (1996) 16502–16513.
[31] M.P. Andersson, P. Uvdal, New scale factors for harmonic vibrational frequencies using the B3LYP density functional method with the triple-ζ basis set 6-311 + G (d, p), J. Phys. Chem. A 109 (2005) 2937–2941.
[32] R.E. Stratmann, J.C. Burant, G.E. Scuseria, M.J. Frisch, Improving harmonic vibrational frequencies calculations in density functional theory, J. Chem. Phys. 106 (1997) 10175–10183.
[33] H. Awada, C. Daneault, Chemical modification of poly(vinyl alcohol) in water, J. Appl. Sci. 5 (2015) 840–850.
[34] N. El-Sawy, M. El-Arnaouty, A.A. Ghaffar, γ-Irradiation effect on the non-cross-linked and cross-linked polyvinyl alcohol films, Polym. Plast. Technol. Eng. 49 (2010) 169–177.
[35] A. Kuanova, Z.A. Nurpeissova, R. Mangazbayeva, K. Park, The obtaining of composite materials based on carboxymethylcellulose and polyvinyl alcohol, Int. J. Biol. Chem. 10 (2017) 62–68.
[36] D. Biswal, R. Singh, Characterisation of carboxymethyl cellulose and polyacrylamide graft copolymer, Carbohydr. Polym. 57 (2004) 379–387.
[37] C.-W. Liew, S. Ramesh, Electrical, structural, thermal and electrochemical properties of corn starch-based biopolymer electrolytes, Carbohydr. Polym. 124 (2015) 222–228.
[38] Y. Zhu, S. Xiao, M. Li, Z. Chang, F. Wang, J. Gao, Y. Wu, Natural macromolecule based carboxymethyl cellulose as a gel polymer electrolyte with adjustable porosity for lithium ion batteries, J. Power Sources 288 (2015) 368–375.
[39] L.T. Cuba-Chiem, L. Huynh, J. Ralston, D.A. Beattie, In situ particle film ATR-FTIR studies of CMC adsorption on talc: the effect of ionic strength and multivalent metal ions, Miner. Eng. 21 (2008) 1013–1019.
[40] V.K. Singh, A. Annu, U. Singh, P. Singh, S. Pandey, B. Bhattacharya, P.K. Singh, Dye sensitized solar cell based on poly (vinyl alcohol) doped with ammonium iodide solid polymer electrolyte, J. Optoelectron. Adv. Mater. 15 (2013) 927–931.
[41] H.S. Mansur, C.M. Sadahira, A.N. Souza, A.A. Mansur, FTIR spectroscopy characterization of poly (vinyl alcohol) hydrogel with different hydrolysis degree and chemically crosslinked with glutaraldehyde, Mater. Sci. Eng. C 28 (2008) 539–548.
[42] U. Riaz, S.M. Ashraf, Characterization of polymer blends with FTIR spectroscopy, characterization of polymer blends: miscibility, Morphol. Interfaces (2014) 625–678.
[43] L. Daniliuc, C. David, Intermolecular interactions in blends of poly (vinyl alcohol) with poly (acrylic acid): 2. Correlation between the states of sorbed water and the interactions in homopolymers and their blends, Polymer 37 (1996) 5219–5227.
[44] S. Kubo, J.F. Kadla, The formation of strong intermolecular interactions in immiscible blends of poly (vinyl alcohol)(PVA) and lignin, Biomacromolecules 4 (2003) 561–567.
[45] L. Guo, H. Sato, T. Hashimoto, Y. Ozaki, FTIR study on hydrogen-bonding interactions in biodegradable polymer blends of poly (3-hydroxybutyrate) and poly (4-vinylphenol), Macromolecules 43 (2010) 3897–3902.
[46] P. Xing, L. Dong, Z. Feng, H. Feng, Miscibility and specific interactions in poly (β-hydroxybutyrate-co-β-hydroxyvalerate) and poly (p-vinylphenol) blends, Eur. Polym. J. 34 (1998) 1207–1211.
[47] M.M. Coleman, D.J. Skrovanek, J. Hu, P.C. Painter, Hydrogen bonding in polymer blends. 1. FTIR studies of urethane-ether blends, Macromolecules 21 (1988) 59–65.
[48] L.N. Sim, S.R. Majid, A.K. Arof, FTIR studies of PEMA/PVdF-HFP blend polymer electrolyte system incorporated with LiCF3SO3 salt, Vib. Spectrosc. 58 (2012) 57–66.
[49] W. Wang, T. Liang, H. Bai, W. Dong, X. Liu, All cellulose composites based on cellulose diacetate and nanofibrillated cellulose prepared by alkali treatment, Carbohydr. Polym. 179 (2018) 297–304.
[50] J.G. Durán-Guerrero, M.A. Martínez-Rodríguez, M.A. Garza-Navarro, V.A. González-González, A. Torres-Castro, J.R. De La Rosa, Magnetic nanofibrous materials based on CMC/PVA polymeric blends, Carbohydr. Polym. 200 (2018) 289–296.
[51] S. Rajendran, M. Sivakumar, R. Subadevi, Investigations on the effect of various plasticizers in PVA–PMMA solid polymer blend electrolytes, Mater. Lett. 58 (2004) 641–649.
[52] A. Alakanandana, A.R. Subrahmanyam, J. Siva Kumar, Structural and electrical conductivity studies of pure PVA and PVA doped with succinic acid polymer electrolyte system, Mate. Today: Proc. 3 (2016) 3680–3688.
[53] H. Nawaz, R. Casarano, O.A. El Seoud, First report on the kinetics of the uncatalyzed esterification of cellulose under homogeneous reaction conditions: a rationale for the effect of carboxylic acid anhydride chain-length on the degree of biopolymer substitution, Cellulose 19 (2012) 199–207.
[54] L. Kuutti, S. Haavisto, S. Hyvarinen, H. Mikkonen, R. Koski, S. Peltonen, T. Suortti, H. Kyllönen, Properties and flocculation efficiency of cationized biopolymers and their applicability in papermaking and in conditioning of pulp and paper sludge,

BioResources 6 (2011) 2836–2850.
[55] M. Krumova, D. Lopez, R. Benavente, C. Mijangos, J. Perena, Effect of crosslinking on the mechanical and thermal properties of poly (vinyl alcohol), Polymer 41 (2000) 9265–9272.
[56] A. Mohamad, N. Mohamed, M. Yahya, R. Othman, S. Ramesh, Y. Alias, A. Arof, Ionic conductivity studies of poly (vinyl alcohol) alkaline solid polymer electrolyte and its use in nickel–zinc cells, Solid State Ionics 156 (2003) 171–177.
[57] C. Ramya, S. Selvasekarapandian, G. Hirankumar, T. Savitha, P. Angelo, Investigation on dielectric relaxations of PVP–NH4SCN polymer electrolyte, J. Non-Cryst. Solids 354 (2008) 1494–1502.
[58] A.M. Stephan, K. Nahm, Review on composite polymer electrolytes for lithium batteries, Polymer 47 (2006) 5952–5964.
[59] N. Rasali, A. Samsudin, Ionic transport properties of protonic conducting solid biopolymer electrolytes based on enhanced carboxymethyl cellulose-NH 4 Br with glycerol, Ionics (2017) 1–12.
[60] H.P. Klug, L.E. Alexander, X-ray diffraction procedures: for polycrystalline and amorphous materials, X-Ray Diffraction Procedures: For Polycrystalline and Amorphous Materials, 2nd ed, by Harold P. Klug, Leroy E. Alexander, pp. 992. ISBN 0-471-49369-4. Wiley-VCH, May 1974., (1974) 992.
[61] R. Jenkins, R.L. Snyder, Diffraction Theory, Wiley Online Library, 2012.
[62] O.W. Guirguis, M.T. Moselhey, Thermal and structural studies of poly (vinyl alcohol) and hydroxypropyl cellulose blends, Nat. Sci. 4 (2012) 57.
[63] F. Abd El-Kader, A. Shehap, M. Abo-Ellil, K. Mahmoud, Relaxation phenomenon of poly (vinyl alcohol)/sodium carboxy methyl cellulose blend by thermally stimulated depolarization currents and thermal sample technique, J. Appl. Polym. Sci. 95 (2005) 1342–1353.
[64] F.A. El-Kader, S. Gaafar, K. Mahmoud, S. Bannan, M.A. El-Kader, Effects of the composition ratio, eosin addition, and c irradiation on the dielectric properties of poly (vinyl alcohol)/glycogen blends, J. Appl. Polym. Sci. 110 (2008) 1281–1288.
[65] Y.G. Andreev, P.G. Bruce, Polymer electrolyte structure and its implications, Electrochim. Acta 45 (2000) 1417–1423.
[66] Y.-C. Lin, K. Ito, H. Yokoyama, Solid polymer electrolyte based on crosslinked polyrotaxane, Polymer 136 (2017) 121–127.
[67] S. Napolitano, A. Pilleri, P. Rolla, M. Wübbenhorst, Unusual deviations from bulk behavior in ultrathin films of poly(tert-butylstyrene): can dead layers induce a reduction of Tg? ACS Nano 4 (2010) 841–848.
[68] A. Saroj, S. Krishnamoorthi, R. Singh, Structural, thermal and electrical transport behaviour of polymer electrolytes based on PVA and imidazolium based ionic liquid, J. Non-Cryst. Solids 473 (2017) 87–95.
[69] J. Bao, X. Qu, G. Qi, Q. Huang, S. Wu, C. Tao, M. Gao, C. Chen, Solid electrolyte based on waterborne polyurethane and poly(ethylene oxide) blend polymer for all-solid-state lithium ion batteries, Solid State Ionics 320 (2018) 55–63.
[70] S. Wang, K. Min, Solid polymer electrolytes of blends of polyurethane and polyether modified polysiloxane and their ionic conductivity, Polymer 51 (2010) 2621–2628.
[71] A.A. Ibrahim, A.M. Adel, Z.H.A. El– Wahab, M.T. Al– Shemy, et al., Carbohydr. Polym. 83 (2011) 94–115.
[72] G.R. Mahdavinia, A. Massoudi, A. Baghban, E. Shokri, Study of adsorption of cationic dye on magnetic kappa-carrageenan/PVA nanocomposite hydrogels, J. Environ. Chem. Eng. 2 (2014) 1578–1587.
[73] M. Shukur, R. Ithnin, M. Kadir, Electrical properties of proton conducting solid biopolymer electrolytes based on starch–chitosan blend, Ionics 20 (2014) 977–999.
[74] K. Meena, K. Muthu, V. Meenatchi, M. Rajasekar, G. Bhagavannarayana, S. Meenakshisundaram, Spectrochimica acta part A: molecular and biomolecular spectroscopy, Spectrochim. Acta A Mol. Biomol. Spectrosc. 124 (2014) 663–669.
[75] G. Prajapati, R. Roshan, P. Gupta, Effect of plasticizer on ionic transport and dielectric properties of PVA–H3PO4 proton conducting polymeric electrolytes, J. Phys. Chem. Solids 71 (2010) 1717–1723.
[76] A. Rajeh, M.A. Morsi, I.S. Elashmawi, Enhancement of spectroscopic, thermal, electrical and morphological properties of polyethylene oxide/carboxymethyl cellulose blends: combined FT-IR/DFT, Vacuum 159 (2019) 430–440.
[77] H.E. Assender, A.H. Windle, Crystallinity in poly (vinyl alcohol). 1. An X-ray diffraction study of atactic PVOH, Polymer 39 (1998) 4295–4302.
[78] M. Isa, A. Samsudin, Potential study of biopolymer-based carboxymethylcellulose electrolytes system for solid-state battery application, Int. J. Polym. Mater. 65 (2016) 561–567.
[79] S. Kumar, G.K. Prajapati, A.L. Saroj, P.N. Gupta, Structural, Electrical and Dielectric studies of nano-composite polymer blend electrolyte films based on (70–x) PVA–x PVP–NaI–SiO_2, Phys. B: Condens. Matter 554 (2019) 158–164.
[80] R. Singh, J. Baghel, S. Shukla, B. Bhattacharya, H.-W. Rhee, P.K. Singh, Detailed electrical measurements on sago starch biopolymer solid electrolyte, Phase Transit. 87 (2014) 1237–1245.
[81] M. Hafiza, M. Isa, Ionic conductivity and conduction mechanism studies of CMC/chitosan biopolymer blend electrolytes, Res. J. Recent Sci., ISSN 2277 (2014) 2502.